Low Temperature Physics/Fizika Nizkikh Temperatur, 2013, v. 39, No. 5, pp. 560–567

Structural evolution of ferromagnetic ^{3}He multilayers adsorbed on exfoliated graphite

T.N. Antsygina and K.A. Chishko

B. Verkin Institute for Low Temperature Physics and Engineering, of the National Academy of Sciences of Ukraine
47 Lenin Ave., Kharkov 61103, Ukraine
E-mail: chishko@ilt.kharkov.ua

Received September 24, 2012

On the basis of our theoretical results describing two-dimensional spin-1/2 Heisenberg model in an external magnetic field we analyze and interpret known from literature experimental data on magnetization of pure ^{3}He monolayers on graphite at ferromagnetic coverages. We clarify the experimentally observed temperature dependences for 2D ^{3}He magnetization under magnetic fields of different magnitude. The cluster size effect in the temperature dependence of the magnetization is studied. We interpret the spin exchange variation in 2D multilayered ^{3}He system during successive promotion of the second, third and fourth layers over first paramagnetic layer strongly coupled with graphite substrate.

PACS: **75.75.–c** Magnetic properties of nanostructures;
67.30.hr Films.

Keywords: multilayered ^{3}He system, 2D spin-1/2 Heisenberg model.

Introduction

Exchange variation with coverage is a characteristic feature of two-dimensional multilayered system of nuclear magnet ^{3}He deposited on planar graphite [1]. The first atomic layer strongly coupled with carbon substrate is paramagnetic. At coverages $\rho > 0.11$ Å^{-2} the promotion of second atomic layer begins. On this stage the second layer is antiferromagnetic with exchange of order a few millikelvins. At $\rho \sim 0.185$ Å^{-2} the second layer is completed and third layer formation with further helium deposition is accompanied by changing of spin exchange in the second layer from antiferro- to ferromagnetic [1]. The ferromagnetic exchange increases with the third layer promotion and reaches a maximum just at completion of the third layer near $\rho \sim 0.24$ Å^{-2} (so-called ferromagnetic anomaly [2]) and then decreases monotonically as the promotion of fourth layer occurs.

It is clear that such a behavior is caused by specific evolution of the multilayer structure. At present, it is generally agreed that namely nuclear spins of second layer solid are responsible for magnetic properties of ^{3}He multilayered system on graphite [3,4]. The thermodynamics of 2D ^{3}He in millikelvin region is completely determined by exchange processes in the subsystem of nuclear spins because at such ultralow temperature the lattice excitations in the helium system with direct interatomic van der Waals interaction of order a few Kelvins are practically frozen. As a result, the second solid ^{3}He monolayer on graphite provides an excellent example of a nearly perfect 1/2-spin nuclear magnet on a triangular lattice. At dense coverages, in ferromagnetic regime, Heisenberg ferromagnetic (HFM) model is quite appropriate to describe magnetic properties of the 2D ^{3}He.

In our previous papers [5,6] we develop the theoretical description of the HFM in an external magnetic field with the aim to interpret experimentally observed magnetic properties of ferromagnetic ^{3}He monolayers on graphite. In this paper we apply the obtained results to clarify the mechanism of exchange evolution with total coverage in multilayered 2D ^{3}He system.

Method

The Heisenberg Hamiltonian is given by

$$H = -J\sum_{\mathbf{f},\delta}\mathbf{S}_{\mathbf{f}}\mathbf{S}_{\mathbf{f}+\delta} - h\sum_{\mathbf{f}}S^z_{\mathbf{f}}, \qquad (1)$$

where $\mathbf{S}_{\mathbf{f}}$ is the spin-half operator at site, $\mathbf{f}$; δ is a vector connecting nearest neighbors on a triangular lattice, $J > 0$.

We use the second-order Green function formalism based on the decoupling of higher Green functions at the second step with introducing vertex parameters to be found. The decoupling scheme is as follows [5]:

$$S_i^\sigma S_j^\sigma S_l^{-\sigma} = \alpha_\perp [\langle S_j^\sigma S_l^{-\sigma}\rangle S_i^\sigma + \langle S_i^\sigma S_l^{-\sigma}\rangle S_j^\sigma],$$

$$S_i^\sigma S_j^{-\sigma} S_l^z = \alpha_z \langle S_i^\sigma S_j^{-\sigma}\rangle S_l^z,$$

$$S_i^z S_j^z S_l^\sigma = [\eta^2 + \alpha_\perp \langle \delta S_i^z \delta S_j^z\rangle] S_l^\sigma,$$

$$i \neq j \neq l, \qquad i \neq l, \qquad \sigma = \pm, \tag{2}$$

where $\alpha_\perp$ and α_z are the vertex parameters, $\eta = \langle S^z\rangle$, and angular brackets mean the thermodynamic averaging. While decoupling the last spin combination we represent S_i^z as $S_i^z = \eta + \delta S_i^z$ and introduce the vertex parameter only in the term containing $\langle \delta S_i^z \delta S_j^z\rangle$.

Another important point is the correct analytical properties of the approximate Green functions for transverse spin components. This condition gives the following equation for order parameter η (magnetization per spin):

$$\eta = \frac{J}{2h\varkappa}\left(\sqrt{\Delta_\perp^2 + \frac{2h^2\tilde{b}_1}{J^2}} - \Delta_\perp\right). \tag{3}$$

Entering here quantities $\Delta_\perp$ and $\tilde{b}_1$ are found from the closed set of equations

$$1 = \frac{2Jc_1}{N}\sum_{\mathbf{k}} g_{\mathbf{k}} + 4\eta^2,$$

$$1 = \frac{2\tilde{b}_1}{\varkappa} - c_1\left[1 - \frac{2J}{N}\sum_{\mathbf{k}}(1-\Gamma_{\mathbf{k}})g_{\mathbf{k}}\right],$$

$$\Delta_\perp = (1-\alpha_\perp)(1-4\eta^2) + \frac{\alpha_\perp}{2\alpha_z}(\Delta_z - 1) +$$

$$+ \frac{J\alpha_\perp c_1}{N}\sum_{\mathbf{k}}(1-\Gamma_{\mathbf{k}})(1-\gamma_0\Gamma_{\mathbf{k}})g_{\mathbf{k}}, \tag{4}$$

where

$$g_{\mathbf{k}} = \frac{\gamma_0}{\omega_{\mathbf{k}}^z}(1-\Gamma_{\mathbf{k}})\coth\left(\frac{\omega_{\mathbf{k}}^z}{2T}\right), \quad \Gamma_{\mathbf{k}} = \frac{1}{\gamma_0}\sum_\delta \exp(i\mathbf{k}\delta),$$

γ_0 is the coordination number,

$$(\omega_{\mathbf{k}}^z)^2 = 2J^2\gamma_0(1-\Gamma_{\mathbf{k}})\ \Delta_z + \gamma_0\tilde{c}_1(1-\Gamma_{\mathbf{k}})\ ,$$

$$\Delta_z = 1 + \tilde{c}_2 - (\gamma_0+1)\tilde{c}_1, \quad \tilde{c}_{1,2} = \alpha_z c_{1,2}.$$

Other quantities, c_1, c_2, α_z, $\alpha_\perp$, $\varkappa$, can be expressed through $\tilde{b}_1$, Δ_z and $\Delta_\perp$. Experimentally measured magnetization $M(T)$ is connected with η by relation $M(T) = 2\eta M_{\rm sat}$ (where $M_{\rm sat} = M(0)$ is the saturation magnetization).

At arbitrary temperature the set of Eq. (4) can be solved numerically. The developed approach allows us to investigate the behavior of thermodynamic quantities at various relations between J and h as well as consider the infinite and finite-sized systems. In particular, in the case of small fields this method gives a proper description of HFM model in the temperature region $h < T < J$, which is very important for interpretation of the experimental data on ^{3}He.

Figure 1 displays the results of our analytical theory for $M(T)/M_{\rm sat}$ of 16×16 triangular lattice Heisenberg ferromagnet at different ratios h/J in comparison with numerical calculations known from literature. It is seen that in the low-field region the results of the present decoupling scheme Eq. (2) demonstrate better agreement with quantum Monte Carlo (QMC) data [7] than those obtained within the scheme employed in our previous paper [6].

The magnetization $M(T)$ of two-dimensional spin system on triangular lattice is principally sensitive to the cluster size $N = L\times L$, especially at small magnetic fields [6]. Figure 2 demonstrates $M/M_{\rm sat}$ as a function of temperature for $h/J = 0.1$ and 0.001 at different N. For a given value of the magnetic field there exists the minimal cluster size N_∞ such that for $N \geq N_\infty$ the magnetization per spin becomes practically independent of N (thermodynamic limit). The smaller is the ratio h/J the larger is N_∞. Thus, at $h/J = 0.1$ the quantity $N_\infty \sim 400$, whereas at $h/J = 0.001$ the value $N_\infty \sim 20000$. The largest N in Figs. 2(a) and (b) are taken to exceed N_∞, so that with further increase in N all dependences $M(T)/M_{\rm sat}$ will coincide with the corresponding upper curves in these graphs.

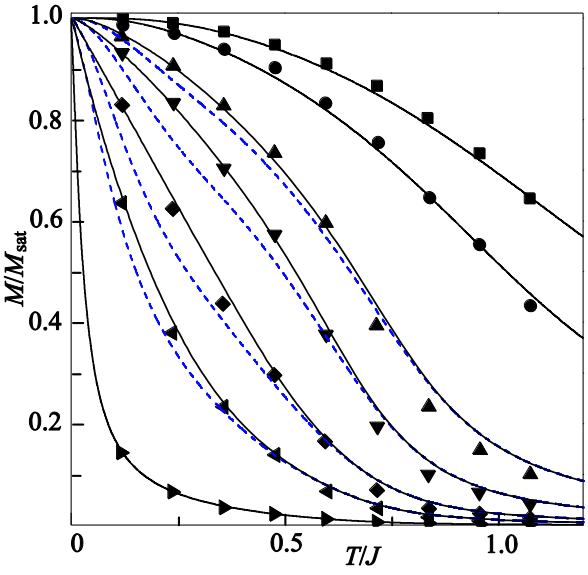

Fig. 1. Temperature dependences of the magnetization for 16x16 triangular lattice HFM at h/J = 0.858, 0.428, 0.0858, 0.0342, 0.0122, $5.52\cdot10^{-3}$, $8.58\cdot10^{-4}$ (from top to bottom): present theory (solid), QMC [7] (symbols), and results of Ref. 6 (dashed).

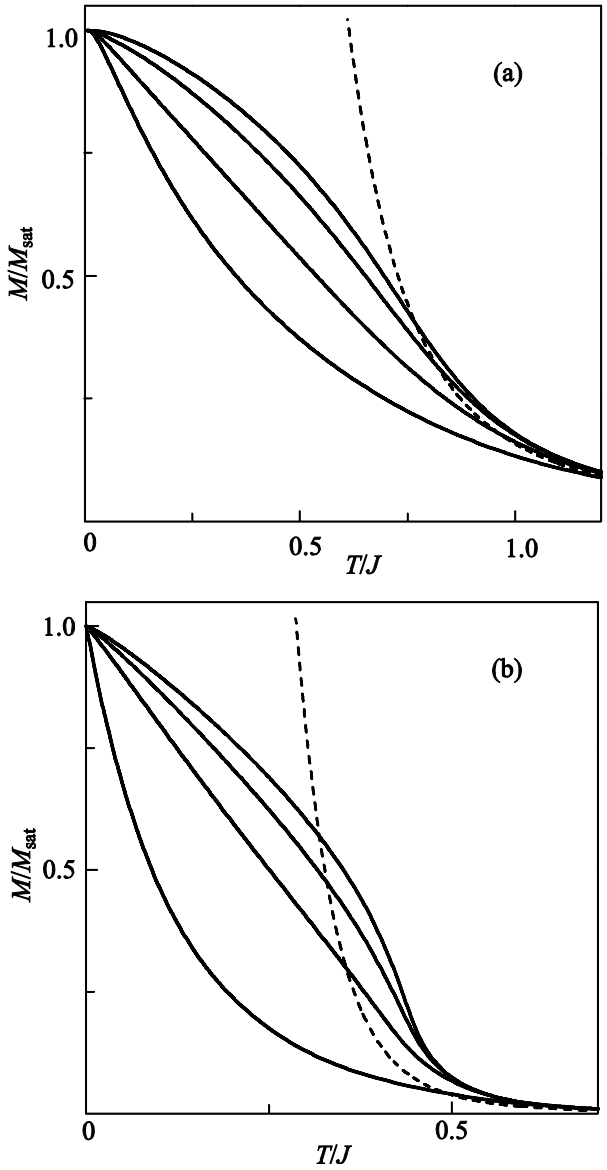

Fig. 2. Magnetization vs temperature at $h/J = 0.1$ (a), 0.001 (b) and different L (from bottom to top): 5, 7, 10, 25 (a), and 25, 50, 75, 150 (b). Present theory (solid), HTSE (dashed).

From Fig. 2 it can be seen that the size dependence of the cluster magnetization is more pronounced in the low-temperature region. With decrease in ratio h/J this region narrows. At $h/J = 0.1$ it begins below $T \sim J$ while at $h/J = 0.1$ the magnetization becomes obviously size-dependent only below $T \sim 0.5J$. Moreover, these are precisely the regions of the most rapid changes of $M(T)/M_{\text{sat}}$ with temperature. This fact is of principal importance when extracting the exchange J from experimental data. Usually, such extraction is made with the help of high-temperature series expansions (HTSE). Since the applicability of HTSE is restricted not only by large N but also by the condition $T > J$, at small fields it describes the magnetization only in a little-informative temperature region, where the value of $M(T)/M_{\text{sat}}$ is several orders less than unity. As a result, in the case of low enough fields the accuracy of extraction of the exchange constant J from the experimental data with the help of HTSE is substantially reduced.

Results and discussion

We calculate the temperature dependence of the magnetization $M(T) = 2\eta M_{\text{sat}}$ and apply the calculations to interpret the experimentally observed magnetic properties of the second solid ^{3}He monolayer on graphite under external magnetic field in view of possible cluster size effects. On this basis the certain conclusions about structural evolution and coverage dependence of the nuclear spin exchange in the system under study will be made.

The saturation magnetization $M_{\text{sat}} = M(0)$ of 2D ^{3}He significantly depends on the coverage and multilayer structure. The quantity M_{sat} is clearly related to the number of active spins involved into ferromagnetic exchange [2,8]. The real measurements of the magnetization cannot be performed at arbitrary low temperatures, so that the direct determination of M_{sat} with high enough accuracy is, as a rule, impossible. To extract this value it is necessary to extrapolate experimental dependences $M(T)$ to the point $T = 0$. Up to now the approximate Kopietz formula [7] has been the only method for carrying out such extrapolation. However, in view of the fact that the validity of this formula is restricted by too narrow region near $T = 0$, an accurate extraction of M_{sat} with its help may break down, especially if available experimental data are beyond the temperature range where the analytical Kopietz expression can be applied with assurance. Furthermore, in the case of small clusters and low external magnetic fields the function $M(T)$ rises sharply near zero temperature (see Fig. 1). This is another factor complicating the reliable extrapolation of $M(T)$ data to $T = 0$. Our analytical results describe correctly the magnetization of 2D HFM in the whole temperature region, so that we can expect to fit the theory and experiment only with use of experimental points for intermediate and high temperatures.

Figure 3 displays the temperature dependences of the magnetization for the second ^{3}He monolayer on an exfoliated graphite at an areal density 23.5 nm^{-2}. The measurements [9] were made on the same sample, so that the sets of the experimental data differ only in the value of the magnetic field, whereas the spin exchange constant J and M_{sat} are common for all the curves. Solid lines in Fig. 3 are the present theoretical results at fixed $J = 1.725$ mK, cluster size $N = 1089$, and different values of B taken in accordance with those used in the experiment. It is seen an excellent agreement between the present theory and experiment at all values of B in the whole temperature range where the measurements were made. Such agreement is a direct evidence in favor of applicability of HFM at this coverage. For comparison, the results for $M(T)$ obtained in Ref. 9 by Kopietz formula at $J = 1.9$ mK and $N = 1000$ are also shown in Fig. 3. It is seen, that this approximation

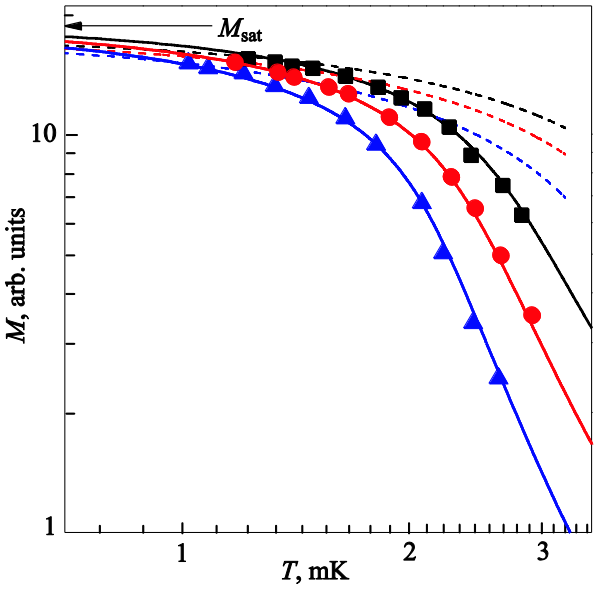

Fig. 3. Temperature dependences of the magnetization for the second ^{3}He monolayer on an exfoliated graphite at B = 113, 56, 26 mT (from top to bottom), $\rho = 23.5$ nm^{-2}. Experimental data [9] (symbols), present theory (solid), results [9] calculated with Kopietz formula (dashed).

is insufficient to describe the temperature region where measurement were made. Besides, as our analysis shows, at $B =$ 56 and 26 mT we deal with finite-sized system so that HTSE is also inappropriate for this case. The quantity N we find to fit the theory to experimental data has a meaning of an averaged cluster size. Another approach is to interpret N as an average size of domains in 2D ferromagnetic coverage of ^{3}He [8]. Anyway, Fig. 3 shows that our theory [5] describes correctly the field dependence of the magnetization of 2D spin system on triangular lattice.

Figure 4 illustrates the experimental [8] and theoretical [5] temperature dependences of the magnetization at fixed magnetic field $B = 14.3$ mT for five different coverages. The exchange J and cluster size N chosen to obtain the best fit of the present theory to the experimental data are shown in Fig. 5. It is seen, that the present theory successively interprets the experiment for all the coverages. As it was shown in Refs. 10, 11 at low ferromagnetic densities such as $\rho =$ 20.5 and 21.5 nm^{-2} the multispin exchange (MSE) effects can contribute to the thermodynamics of solid ^{3}He monolayers. For these two coverages there exist experimental measurements [8] at temperatures up to 5.5 mK, so that in this case we can check up the applicability of HFM in a wider temperature range (see Fig. 4(b)). Figure 4(b) displays the corresponding dependences $M(T)$ completed by the high-temperature data. To draw solid lines in Fig. 4(b) we take precisely the same values of J and N as in Fig. 4(a) at $T < 3$ mK. From Fig. 4(b) it is seen that the present theoretical results and experimental data are in close agreement not only at low but also at high tempera-

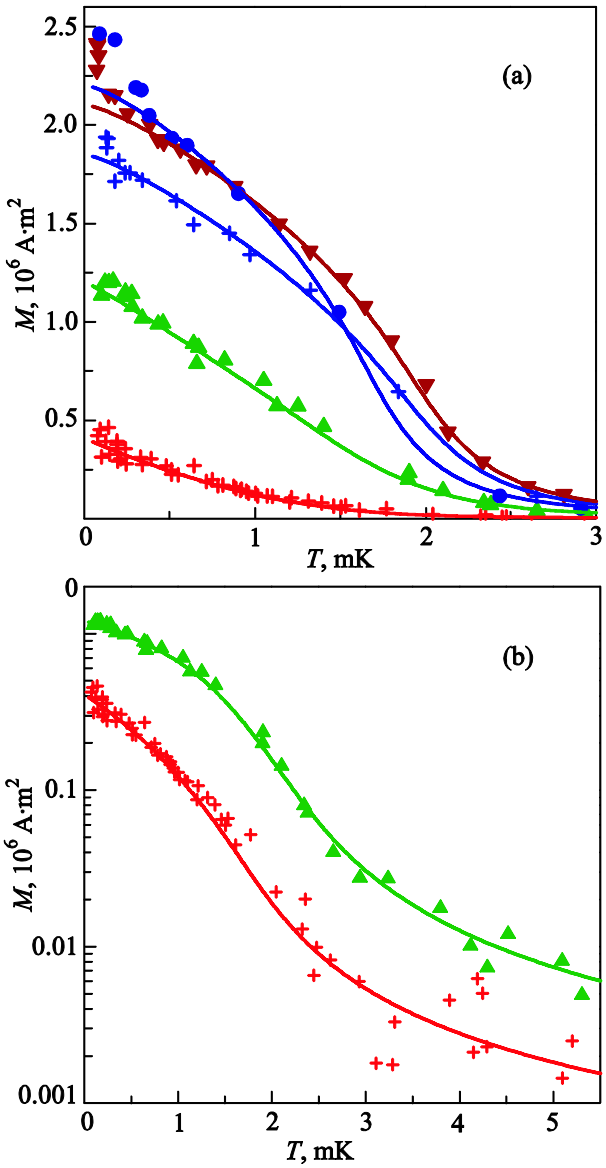

Fig. 4. Temperature dependences of the magnetization for the second ^{3}He monolayer on an exfoliated graphite at B = 14.3 mT and (from bottom to top): $\rho =$ 20.5, 21.5, 22.7, 24.8, 25.9 nm^{-2} (a), and $\rho =$ 20.5, 21.5 nm^{-2} in extended temperature range (b). Experimental data [8] (symbols), present theory (solid).

tures. This suggests that the behavior of $M(T)$ at $\rho =$ = 20.5 and 21.5 nm^{-2} can be treated with the help of HFM. In Ref. 11 it was shown that a pure Heisenberg behavior is observed at $\rho \geq 22$ nm^{-2} when the exchange constants J_c and J_χ inferred, respectively, from HTSE heat capacity and susceptibility data coincide (see Fig. 4 in Ref. 11). At $\rho =$ 21.5 and 20.5 nm^{-2} effect of MSE makes itself evident in slight difference between J_c and J_χ [11]. Such conclusions were made on the basis of HTSE calculations for an infinite MSE model in zero field. However, at coverages $\rho =$ 21.5 and 20.5 nm^{-2} we deal with finite-sized systems under external magnetic field. To estimate properly the multiple-spin contribution in this case it is necessary to

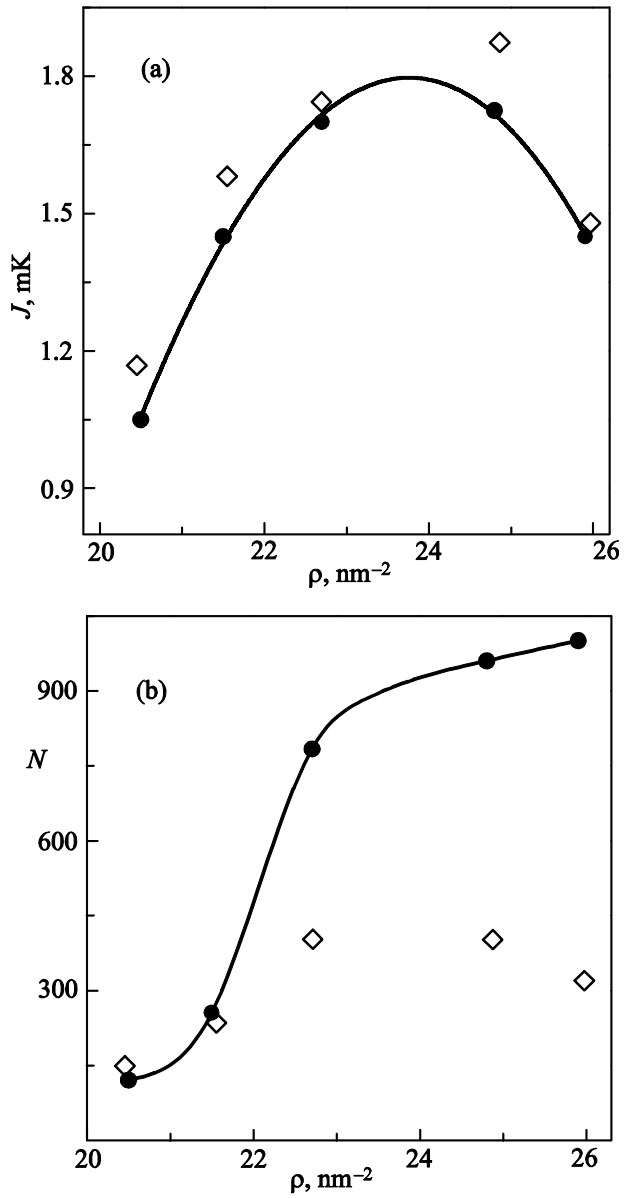

Fig. 5. Exchange J (a) and cluster size N (b) as functions of coverage ρ that give the best fit of the theory (●) to the experimental data [8]. The polynomial approximations (solid) and the results of Ref. 8 (◇). Solid lines are drawn by eye.

have the solution of MSE model at these specified conditions.

Figure 5 presents the variation of the exchange constant J and cluster size N with total coverage. In Fig. 5(a) the nonmonotonic behavior of $J(\rho)$ is seen, when with increase in coverage the exchange constant first increases, goes through a maximum, and then decreases. Cluster size N is found to increase monotonically with density (see Fig. 5(b)). From our analysis it follows that at $\rho \gtrsim 23$ nm^{-2} the thermodynamic limit is already reached, $M(T)/N$ is independent of N, and the ^{3}He second monolayer behaves like an infinite homogeneous ferromagnet, as it should be at such densities. At low coverages clusters are small, and strong spin fluctuations near their boundaries affect significantly the exchange reducing the average value of J [2,12]. As the cluster increases in size, the fraction of spins near its boundary decreases. This diminishes the boundary effects leading to a rise in the average exchange constant. When the thermodynamic limit is reached, the role of the boundaries becomes insignificant, and the value of J is completely determined by processes within the cluster.

The saturation magnetization behaves with ρ in a similar way as $N(\rho)$ (see Fig. 6). The grafoil surface used in the experiment [8] was composed of atomically smooth platelets with linear size about 100 Å. From Fig. 5(b) one can see that at $\rho = 25.9$ nm^{-2} only one ferromagnetic island can be placed on a typical platelet. The ratio between number of clusters at given ρ and number of clusters at $\rho = 25.9$ nm^{-2} is shown in Fig. 6. It demonstrates the tendency of the cluster formation. At first with increasing coverage the number of clusters increases, then decreases showing that the clusters merge to become a homogeneous ferromagnetic system.

The treatment of the experimental data in Fig. 4 with the Kopietz approximate formula leads to the following findings [8]. Entering this formula quantity N is usually identified with an effective cluster size. It behaves similarly to $J(\rho)$ first increasing with ρ and then decreasing (open diamonds in Fig. 5). As noted in Ref. 8, this result contradicts to the experimentally observed continuous growth of the saturation magnetization with density, which implies an increase in the number of ferromagnetic spins, and, consequently, the growth of the cluster size. In our opinion, such inconsistency in the estimation of N is due to the fact that the Kopietz formula is appropriate at rather low temperatures. An attempt to apply this formula to the

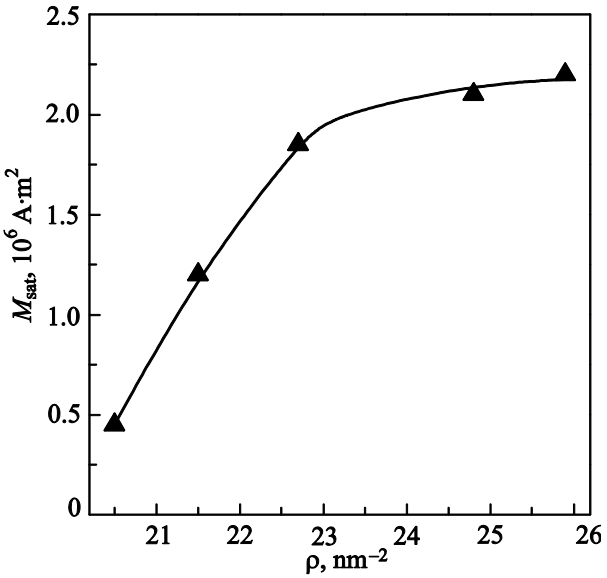

Fig. 6. The coverage dependences of the saturation magnetization (▲). Symbols are the result of fit to the experimental data [8]. Solid line is drawn by eye.

experimental data in as wide temperature range as possible results in an inaccurate estimate for N.

Figure 7 demonstrates the temperature dependences of the magnetization measured by different groups of experimentalists [2,14–16]. The results are obtained at various magnetic fields from high enough (113 mT) till very small (0.35 mT). In the case of two highest fields the measurements were made at dense coverages (large N) in a wide temperature range, including the region where the magnetization is close to saturation as well as temperatures $T/J \gg 1$ where HTSE applies. This made it possible to extract the values of J and $M_{\rm sat}$ combining the Kopietz formula and HTSE [2]. The quantities J and $M_{\rm sat}$ found with the help of such procedure agree very well with the results of the present calculations. In particular, for $B = 113$ mT we obtain exactly the same value of exchange constant J = 2.8 mK. Note, that the measurements at $B = 113$ mT were taken at very high density $\rho = 38$ nm^{-2} when the third layer is considerably filled with ^{3}He atoms. The applicability of the 2D Heisenberg model for this case is discussed in Ref. 2.

At B = 14.21 and 6.44 mT there is a lack of low-temperature experimental data, so that the Kopietz formula gives no way for deducing $M_{\rm sat}$ with acceptable accuracy. As a result, the exchange constant cannot be extracted definitely from HTSE. The situation with $M(T)$ at B = 0.35 mT is even more complicated. The corresponding measurements

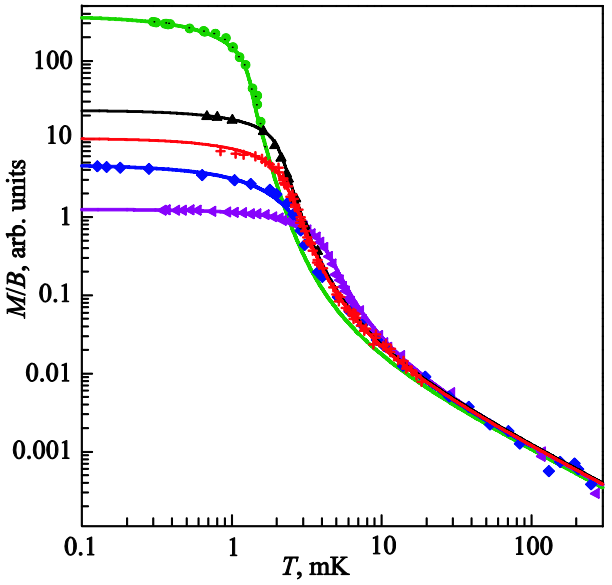

Fig. 7. Temperature dependences of 2D ^{3}He magnetization in ferromagnetic regime. Experimental results (symbols) at (from top to bottom): $B = 0.35$ mT, $\rho = 24.2$ nm^{-2} (Ref. 16); $B = 6.44$ mT, $\rho = 23.3$ nm^{-2} (Ref. 14); $B = 14.21$ mT, $\rho = 23.3$ nm^{-2} (Ref. 15); $B = 30.5$ mT, $\rho = 24.4$ nm^{-2} and $B = 113$ mT, $\rho = 38$ nm^{-2} (Ref. 2). Present theoretical curves (solid) are fitted at (from top to bottom): J = 1.65 mK, N = 10000; J = 2.1 mK, N = 2500; J = 2.05 mK, N = 529; J = 2.15 mK, N = 144; J = 2.8 mK, N = 256.

were made at $h \ll T < J$, and neither HTSE nor Kopietz formula are applicable. On the contrary, the present theory is suitable to interpret these experiments. The best fit to the experimental data for $B = 0.35$ mT gives $N = 10^4$. The obtained cluster size, even if very large, does not correspond to an infinite system due to extremely small magnetic field $h/J \sim 10^{-4}$.

Figure 5(b) shows that the cluster size N monotonically increases with coverage and the saturation magnetization behaves with ρ in a similar way (see Fig. 6). It means that saturation magnetization is in direct proportionality with the number of ferromagnetically coupled spins. Both curves, $N(\rho)$ and $M_{\rm sat}(\rho)$ have a characteristic two-stage form. The first stage (at $\rho \lesssim 23.5$ nm^{-2}) with relatively high values of derivatives $\partial N/\partial\rho$ and $\partial M_{\rm sat}/\partial\rho$ changes to the coverage dependence with rather moderate slope just at $\rho \gtrsim 23.5$ nm^{-2} corresponding to the third layer completion [1] and beginning of the fourth layer promotion. The function $M_{\rm sat}(\rho)$ (Fig. 6) is in close agreement with experimental dependence $M_{\rm sat}(\rho_3)$ given in Ref. 13 (ρ_3 is the density of the third layer). Thus, we conclude that our results support the model of ^{3}He second layer in ferromagnetic regime proposed in Ref. 13 (see also Ref. 8). The second layer becomes ferromagnetic during development of third-layer islands over completed second one. The presence of third-layer spot of average size N under the corresponding group of second-layer spins produces an additional local compression of the underlying 2D solid due to surface tension under overlying spot and then suppress to a some degree the intralayer exchange in the second layer because an external pressure reduced exchange in the spin system [1,17]. On the other hand, during third layer formation the overlayer islands are involved into to three-spin interlayer permutations which leads to the ferromagnetism [17] in the bilayered system. The proportional to N average size of the ferromagnetic islands grows with total coverage ρ and, correspondingly, J and $M_{\rm sat}$ increase within the ferromagnetic regime as the total coverage ρ increases. As a result, the maximum of exchange is reached exactly at $\rho = 24$ nm^{-2} where of the third layer is just completed. At $\rho >$ 24 nm^{-2} the fourth layer (presumable, liquid) becomes to be promoted and the number of active spins continuous increase as it is evident from behavior of $M_{\rm sat}(\rho)$ (Fig. 5(b) and Fig. 6). The local consolidation of the third layer due to surface tension from fourth-layer islands leads to suppression the exchange frequencies in the system, but the number of magnetically active spins slowly increases because of formation of the low-exchange ferromagnetic regions in the third layer under adjacent fourth-layer spots. This fact is clearly illustrated by magnetization curve belonging to the coverage $\rho = 25.9$ nm^{-2} in comparison with those at $\rho = 24.8$ nm^{-2} (see Fig. 4). The first curve lies below the second one practically in the whole temperature region, except of the narrow low-temperature interval where the first dependence

increases rapidly and reaches the value of M_{sat} which contains contributions not only from second-layer ferromagnet, but also from third-layer low-exchange subsystem. Moreover, the curve of M_{sat} at $\rho = 24.8$ nm^{-2} demonstrates the same rapid increase at $T \to 0$, although in this region it lies lower than previous one. Such behavior of magnetization at the dense coverages is evidently connected with the presence of fourth-layer islands. It should be noted that from this point of view the mentioned behavior of $M(T)$ can be interpreted without proposed in Ref. 8 of a magnetic phase transition in the layered ^{3}He system at very low temperatures.

On the other hand, at beginning of the second layer promotion (at $\rho > 11$ nm^{-2}) over the first layer strongly coupled with graphite substrate it evaluates at ultralow temperature as a set of compact islands where only ring in-plane permutations are possible. Interplane permutations between first and second layers are depressed because of with strong attraction of the first-layer atoms to the graphite substrate. As a result, the many-particle (four, five, six, etc.) in-plane ring permutations lead to antiferromagnetic exchange in the ^{3}He 2D nuclear magnet on triangular lattice [10,11,18,19], and the mentioned permutations are more probable near the boundaries of islands. As the total coverage ρ increases within the second layer promotion (11 nm$^{-2} < \rho <$ 18 nm^{-2}), the islands grow and the antiferromagnetic exchange increases up to the moment when the islands become coalescing and the antiferromagnetic exchange decreases with decrease of islands boundary regions and formation of third layer nuclei responsible for ferromagnetic contribution to the exchange processes. With further decrease in ρ the ferromagnetism becomes predominant.

Another noticeable feature of the system under study is that the coincidence of the experimental dependence $M(T)$ with the theory can be obtained (at given coverage ρ) only at determined average cluster size N. It means that at least in ferromagnetic regime the 2D ^{3}He multilayered system consists of practically independent nanoclusters. This fact is in a certain contradiction with common assumption about possible domain structure of 2D helium in ferromagnetic regime [8]. The alternative explanation is that an average cluster size is the size of third-layer islands which are responsible for three-spin ferromagnetic exchange in the system. During promotion of the third island-like layer the spots under second layer grow and the number of ferromagnetic spins increases proportionally. Finally, the third layer is completed, and the described process will be repeated by fourth island-like layer under completed third one, but with reduced $\partial N/\partial\rho$ in view of smaller interaction of fourth-layer atoms with substrate (third layer) as compared to the interaction of the third-layer atoms with their substrate (second layer).

Conclusions

The analytical approach for the 2D ferromagnetic Heisenberg model in an external magnetic field developed in Ref. 5 which describes properly the thermodynamics of infinite and finite-sized spin systems at arbitrary temperatures and fields is applied in the present paper to interpret the experimentally observed exchange evolution in ^{3}He multilayers on graphite depending on total coverage of helium deposit. We give a consistent interpretation to a great number of experimental data on magnetization of ^{3}He monolayer on graphite and ^{3}He on ^{4}He-preplated graphite in the ferromagnetic regime. Fitting the present theory to the experimental data we extract the exchange constant J, saturation magnetization M_{sat}, and average cluster size N at given h. Below the thermodynamic limit the shape of magnetization curves $M(T)/M_{sat}$ at $h/J \ll 1$ is found to be extremely sensitive to the cluster size just in the temperature region $h < T < J$. Due to the proper description of the magnetization for finite-sized systems at intermediate temperatures, the proposed theory provides an unambiguous extraction of N from the experimental data.

For pure ^{3}He on graphite we succeed in interpretation of experimental data for magnetization $M(T)$ measured on the same sample at the fixed coverage for different values of the magnetic field. Under this condition J and N are the same for all dependences $M(T)$. Once the values of J and N are identified, each theoretical curve $M(T)$ at given B falls precisely on the corresponding experimental points. An excellent agreement between the theory and experiment is a direct evidence in favor of applicability of the Heisenberg model. We also interpret the behavior of experimentally obtained magnetization curves $M(T)$ at fixed B and different coverages. Although the Heisenberg model is found to be appropriate at $\rho \geq$ 22.0 nm^{-2} [11], we show that it provides a reasonable description for $M(T)$ at $\rho =$ 20.5 and 21 nm^{-2}. On the basis of these results, the coverage dependences of the exchange constant, saturation magnetization, and average cluster size are obtained and analyzed. The exchange constant displays non-monotonic behavior with increasing coverage. It first increases, goes through a maximum, and then decreases. The cluster size N as well as M_{sat} continuously grow with total coverage.

When interpreting experimental results, we have found that characteristic behavior of the dependences $M_{sat}(\rho)$ and $N(\rho)$ are unambiguously correlated with known stages [1] of ferromagnetic ^{3}He multilayer formation. It gives us possible to make conclusions exchange evolution during multilayered grown of 2D ^{3}He on graphite. The ferromagnetic exchange appears due to contribution of interlayer three-particle permutations during promotion of third-layer islands over completed second layer. With third-layer promotion the excessive pressing from overlayer islands suppresses antiferromagnetic intralayer exchange in the

second-layer solid, so that three-spin ferromagnetic exchange becomes predominant. The exchange constant reaches its maximum just at completion of third layer.

1. D.S. Greywall, *Phys. Rev. B* **41**, 1842 (1990).
2. E. Collin, C. Bäuerle, Yu.M. Bunkov, and H. Godfrin, *Phys. Rev. B* **73**, 125421 (2006).
3. T.N. Antsygina and K.A. Chishko, *J. Low Temp. Phys*. **119**, 677 (2000).
4. H. Fukuyama, *J. Phys. Soc. Jpn*. **77**, 111013 (2008).
5. I.I. Poltavsky, T.N. Antsygina, M.I. Poltavskaya, and K.A. Chishko, *Physica B: Condens. Matter* **407**, 3925 (2012).
6. T.N. Antsygina, M.I. Poltavskaya, I.I. Poltavsky, and K.A. Chishko, *Phys. Rev. B* **77** 024407 (2008).
7. P. Kopietz, P. Scharh, M.S. Skaf, and S. Chakravarty, *Europhys. Lett*. **9**, 465 (1989).
8. P. Schiffer, M.T. O'Keefe, D.D. Osheroff, and H. Fukuyama, *J. Low Temp. Phys*. **94**, 489 (1994).
9. C. Bäuerle, Yu.M. Bunkov, S.N. Fisher, and H. Godfrin, *Czech. J. Phys*. **46**, Suppl. S1, 403 (1996).
10. M. Roger, C. Bäuerle, H. Godfrin, L. Pricoupenko, and J. Treiner, *J. Low Temp. Phys*. **112**, 451 (1998).
11. M. Roger, C. Bäuerle, Yu.M. Bunkov, A.-S. Chen, and H. Godfrin, *Phys. Rev. Lett*. **80**, 1308 (1998).
12. P. Schiffer, M.T. O'Keefe, D.D. Osheroff, and H. Fukuyama, *Phys. Rev. Lett*. **71**, 1403 (1993).
13. H. Godfrin, R.E. Rapp, K.-D. Morhard, J. Bossy, and C. Bäuerle, *Phys. Rev. B* **49**, 12377 (1994).
14. H. Godfrin, R.R. Ruel, and D.D. Osheroff, *Phys. Rev. Lett*. **60**, 305 (1988).
15. H. Godfrin, R.E. Rapp, and D.D. Osheroff, *Physica A* **163**, 101 (1990).
16. H.M. Bozler, Yuan Gu, Jinshan Zhang, K.S. White, and C.M. Gould, *Phys. Rev. Lett*. **88**, 065302 (2002).
17. A. Abragam and M. Goldman, *Nuclear Magnetism: Order and Disorder*, Clarendon Press, Oxford (1982).
18. H. Godfrin and R.E. Rapp, *Adv. Phys*. **44**, 113 (1995).
19. M. Roger, *Phys. Rev. B* **56**, R2928 (1997).